Advances in Water Resources 183 (2024) 104589

Contents lists available at ScienceDirect

Advances in Water Resources

journal homepage: www.elsevier.com/locate/advwatres

Pre-asymptotic dispersion revisited

Deviyani Gurung, Mohammad Aghababaei, Timothy R. Ginn *

Civil and Environmental Engineering, 101 Sloan Hall, Pullman, 99163, WA, USA

ARTICLE INFO

Keywords:
Pre-asymptotic dispersion
Advection–dispersion
Transport

ABSTRACT

We develop a new approach to formulation and solution of mathematical models of one-dimensional advective–dispersive transport that specifies the hydrodynamic dispersion coefficient as a function of time since the solute has entered the flow field, termed 'age.' This approach addresses Taylor's concern about the use of time-dependent dispersion coefficients to model pre-asymptotic dispersion by replacing time-dependence with age-dependence, where age of solute is exposure-time to the flow. We show closed form solutions obtained for transport on the $-\infty < x < \infty$ and a numerical solution for transport on the $0 < x < \infty$ domain. We demonstrate how this works by application to an in-silico experiment recently published in a study addressing the same issue in a different manner. Our simple and intuitive approach matches the simulated pre-asymptotic data without additional terms or parameter fitting. The same principle applies to pre-asymptotic dispersion in other important upscaled one-dimensional transports e.g., in river corridor or groundwater flows.

1. Introduction

One-dimensional advective–dispersive transport in many types of steady flows can be described with a mass balance expression that uses a constant dispersion coefficient provided that sufficient time has transpired since commencement of transport. This foundation is due to Taylor (1953, 1954), and interpreted using solute spatial moments in Aris (1956) for flow in a tube. Applications are ubiquitous involving any steady nonuniform flow typically involving shear imparting an early time deformation of uniform initial solute pulses (for initial value problems), or solute within boundary injections (for boundary value problems) that are eventually erased by lateral displacements. In many situations the time required to reach such asymptotic conditions is large with respect to the observation time scale (Smith, 1981) for instance in natural streams (Fischer, 1967), and in porous media (Corey et al., 1970). Thus many authors have sought upscaled one-dimensional transport models that can represent pre-asymptotic through asymptotic conditions, via an effective and dynamic longitudinal dispersion coefficient. Numerous studies have reported on how to express the effective one-dimensional longitudinal dispersion coefficient of a solute in a given steady flow field to reflect the pre-asymptotic conditions, as well as the temporal or spatial scale over which pre-asymptotic conditions persist, (e.g., Gill (1967), Gill and Sankarasubramanian (1970), Fried and Combarnous (1971), Smith (1981), Guven et al. (1984), Dagan (1984), Han et al. (1985), Seo and Cheong (1998), Dentz and Carrera (2007), Wang et al. (2012) and Taghizadeh et al. (2020)). The mathematical approaches used to derive the effective 1-D longitudinal dispersion coefficient vary, but most of the foregoing works involve the following basic steps of analyses. A two- or three-dimensional flow field, often in a conduit such as a pipe, fracture, river channel, or aquifer, is specified mathematically; the "microscopic-scale" transport equation for a solute (typically a point source or a source that spans a plane perpendicular to the mean flow direction) transported by this flow field is solved explicitly; and finally the effective dispersion coefficient, defined by construction of the upscaled 1-D transport model as one-half of the time derivative of second centered spatial moment of the solute plume, is derived. The 1-D model typically is designed to simulate the cross-sectional average concentration in the conduit as a function of downstream distance and time.

The resulting upscaled one-dimensional dispersion coefficient is typically expressed in the form [e.g., Eq. (79) in Dentz and Carrera (2007) or Eq. (28) in Wang et al. (2007)] $D(t; v, D_m) = D_m + c_0 \frac{v^2}{D_m} \cdot \sum_{n=1}^{n=\infty} c_n f(n, t, D_m)$, where t is time, v is steady macroscopic (mean) velocity, D_m is the molecular diffusion coefficient for the solute in static water, c_0 and c_n are constants, and f is a function typically involving exponentials with arguments that are products of t, D_m, and powers of n. This detail reveals that these expressions are linear in mean velocity squared so that if velocity is zero then the derived diffusion coefficient is no longer time dependent and reduces to D_m.

Limitations on the use of this approach include the assumptions of: steady flow; an explicit representation of the flow field (either deterministically or stochastically); a diagonal diffusion (or microdispersion (Dentz and Carrera, 2007)) tensor in the microscopic-scale

* Corresponding author.
E-mail address: tim.ginn@wsu.edu (T.R. Ginn).

https://doi.org/10.1016/j.advwatres.2023.104589
Received 5 April 2023; Received in revised form 15 November 2023; Accepted 21 November 2023
Available online 14 December 2023

transport model; and often mathematical assumptions introduced per the method used to obtain $D(t; v, D_m)$, e.g., that the longitudinal gradient of the cross-sectional averaged solute concentration be much greater than that of the microscopic concentration fluctuations (Wang et al., 2012).

Henceforth we simplify the notation to $D(t)$ where t is time since solute entered the flow field. Some authors use $D(x)$ where x is distance traversed by the solute, in which case pre-asymptotic dispersion is termed "scale-dependent.' The temporal scale of pre-asymptotic transport in any given flow is typically found in terms of a characteristic time (or space) scale for solutes to fully experience the complete distributions of transport velocities, e.g., pipe radius squared divided by molecular diffusion coefficient in pipe flow (e.g., Gill and Sankarasubramanian, 1970), river depth squared divided by lateral dispersion coefficient (e.g., Wang et al., 2012) or spatial scale of velocity fluctuations divided by lateral dispersion coefficient in porous media, (e.g., Dentz et al., 2000). Corresponding spatial scales are obtained by multiplying these temporal scales by mean velocity (e.g., Dagan, 1987; Fischer, 1967). More general studies examine nonlocal forms for dispersive flux in more complex transport scenarios. Here we restrict our attention to local forms.

The resulting equation for the simplest 1D steady flow case is often written with $D(t)$, as

$$\frac{\partial c}{\partial t} + v\frac{\partial c}{\partial x} - D(t)\frac{\partial^2 c}{\partial x^2} = 0 \tag{1}$$

with either the semi-infinite space domain $x > 0$ for boundary value formulation or the infinite domain $-\infty < x < \infty$ and with appropriate initial conditions in either case. A solution to (1) for all $t > 0$ by Gill and Sankarasubramanian (1970) involves a series in space derivatives (hinting at later non-local theories) with truncation to two terms of the series found often suitable. Pasmanter (1985) study a range of transport problems in 3-D via Lie algebra (often involving wavevector power series expansions) and note the approximate nature of several outstanding 1-D solutions. Of the numerous other works on closed-form 1-D solutions we mention the remarkably poorly-cited Warrick et al. (1972) who solve the initial value problem including an independently transient velocity and Barry and Sposito (1989) who give a quasi-implicit solution for the boundary value problem requiring solution of Volterra integral equations of the 2nd kind. Efforts to find simpler solutions to the 1-D boundary value problem continue unsuccessfully, foreshadowed by Warrick et al. (1972) who warn that a solution to the boundary value problem may not exist, and with some controversy, e.g., Deng and Qiu (2012). Thus it is unsurprising that most studies involving boundary value problems on $x > 0$ with either time- or space-dependent dispersion coefficients seek to approximate these as initial value problems on $-\infty < x < \infty$, for which closed-form solutions are more readily available. The associated errors in this approximation depend on Péclet number, e.g., Charbeneau (2000), Gurung and Ginn (2020), and so numerical solutions are often required.

Taylor critiqued the notion of time-dependent dispersion coefficients "$D(t)$" (Taylor, 1959; Smith, 1981; Taghizadeh et al., 2020) stating "It seems to me that this is an illogical conception... If therefore you attempt to analyze the distribution of concentration from two sources which started at different times by this method, it would be necessary to assume, in places where the distributions overlapped, that the diffusion constant had two different values at the same time and at the same point in space". Taghizadeh et al. (2020) show (Section 9, 1st paragraph) that Taylor's paradox corresponds to a problem with superposition of solutions for solute distributions emanating from different start times, because a time-dependent dispersion coefficient would necessarily have multiple values at a given point in (x, t) for a transport equation applied to a single space–time coordinate system with a singly-defined origin in time. The same paradox arises when dispersion coefficients depend on scale or space traversed and expressed as $D(x)$ (Pickens and Grisak, 1981; Dagan, 1987; Yates, 1992; Gelhar, 1993; Pérez Guerrero and Skaggs, 2010) when solutes start at different locations, e.g., in the case of diffusive release of a solute from sediments along a river reach.

We emphasize two important points: first, when boundary and initial conditions involve only one release location and one time, Taylor's critique does not apply; second, when multiple releases occur over time, or at multiple locations, one may solve the problem with pre-asymptotic dispersion numerically by calculating the solute concentration distribution emanating from each source (using, respectively, $D(x)$, or $D(t)$), and then adding these respective solutions over all (x, t), as long as no nonlinear biochemical transformations are involved. That is, while one may not be able to write a single governing equation for the complete solute distribution, one may still superpose numerical solutions for a strictly passive tracer. We pursue our alternative formulation because the challenge of writing a single governing equation including pre-asymptotic dispersion for the case of multiple solute release times *and* locations remains, doing so gives rise to closed-form solutions in some cases, such a form will be necessary if one wishes to include nonlinear reaction kinetics endured by the solute(s), and solving separately for the solute distribution from each release may become computationally intensive.

By including an independent variable that keeps track of age (exposure-time) of solute to the flow field (following the approach of Ginn (1999) and Ginn and Schreyer (2023)), "ω", we can write the dispersion coefficient as "$D(\omega)$" instead of as $D(t)$. Doing so eliminates Taylor's concern both mathematically and conceptually, because the dispersion coefficient will now be singly defined in time, space and age. Here we illustrate the structuring of simple 1-D transport equations on age to accommodate pre-asymptotic dispersion and provide simple closed-form solutions for both initial and boundary value problems specified on the space domain $-\infty < x < \infty$; i.e., when upstream diffusive transport is allowed. For the case where the space domain is restricted to $0 < x$ and upstream migration is not allowed we are so far unable to find a closed-forms solution, but the same formulation (1) provides a basis for numerical solution as will be shown.

The paper is organized as follows. In Section 2 we review the conceptual and theoretical framework of exposure time structured transport equations. In Section 3 we present the closed-form solutions for the $-\infty < x < \infty$ case for both initial and boundary value problems. In Section 4 we introduce the target data of Taghizadeh et al. (2020) and apply our closed-form solution to simulate that initial value problem. In Section 5 we demonstrate the numerical solution of our model to solve a boundary value problem on $0 < x$ where no upstream transport is allowed. In Section 6 we discuss the implications of these results.

2. Age-structured transport

General mass balance expressions for solutes or suspensions undergoing transport in $(\boldsymbol{x}, t)$ can be extended to include an additional dimension ω to keep track of exposure-times of solutes or suspensions to the transport domain Ginn (1999) including oceans (Delhez et al., 1999), or to other solutes (Gurung and Ginn, 2020), surfaces (Ginn, 1999), diffusive transport domains (in mobile-immobile mass transfer (Ginn, 2009; Ginn et al., 2017)), or to discrete compartments in general compartment modeling (Ginn and Schreyer, 2023). In the context of (1) then $c(x, t)$ becomes a distribution $c(x, t, \omega)$ over ω that represents exposure-time (or simply "age") of c to the flow field. The aging of mass in a conservation equation is done by an advection term with the rate (velocity) of aging given by an age velocity v_ω. Doing so and replacing the time-dependence of D with ω-dependence gives

$$\frac{\partial c}{\partial t} + v_\omega\frac{\partial c}{\partial \omega} + v\frac{\partial c}{\partial x} - D(\omega)\frac{\partial^2 c}{\partial x^2} = 0 \tag{2}$$

Just as the material velocity component in direction x is defined as $v = \Delta x/\Delta t$ on a physical streamline, the aging velocity in direction ω

is defined as $v_\omega = \Delta\omega/\Delta t$. Throughout this paper the aging velocity $v_\omega = 1$, so the material motion in the ω direction obeys $\Delta\omega = \Delta t$. Thus e.g. mass in the flow field ages (moves by advection) by one second $\Delta\omega$ per second Δt. In this case of unit aging velocity the age dimension can be viewed as a local time coordinate, with origin shifted to the start time of solute exposure to the flow field, $t_o = t - \omega$. Non-unity aging velocities can be specified for useful application in other areas such as dose kinetics (Sengör et al., 2009) or population dynamics (Ginn and Loge, 2007). As long as the velocity of aging v_ω is not a function of age itself, transport by a divergence-free velocity field remains divergence free in the extended coordinate system (Ginn, 1999).

Writing the boundary and initial conditions for particular instances is straightforward: in initial value problems the initially present solute is specified as a function of space, at zero age and time, and in boundary value problems the influent solute enters the domain as a function of time, at influent boundaries and at zero age (no matter whether Dirichlet, Neumann, or Robin boundary condition is specified). The age-structured solution to this sort of equation, $c(x,t,\omega)$, is then integrated over ω to recover the final solution $c_T(x,t)$. That is, solution of (2) gives the distribution of mass concentration over age ω at any point in the space and time domain, expressed as $c(x,t,\omega)$. The concentration that one observes and measures at that point in space and time, $c_T(x,t)$ is the total mass of this distribution, given by the integration $\int_0^\infty c(x,t,\omega)d\omega$. If all initial mass at $t = 0$ also starts out at zero age ($\omega = 0$), then this integration is equal to $\int_0^t c(x,t,\omega)d\omega$.

3. Solutions for the $-\infty < x < \infty$ domain

We presume that one-dimensional flow occurs at constant velocity over the entire line $-\infty < x < \infty$ and solute is injected at $x = 0$, as in one-dimensional approximation of tracer tests in rivers or pipes, and we include first-order decay with rate coefficient that may also depend on solute age to the flow field, $\lambda(\omega)$. Then Eq. (2) becomes

$$\frac{\partial c}{\partial t} + v_\omega\frac{\partial c}{\partial \omega} + v\frac{\partial c}{\partial x} - D(\omega)\frac{\partial^2 c}{\partial x^2} = -\lambda(\omega)c;\ -\infty < x < \infty, 0 < t,\ 0 < \omega, \quad (3)$$

We now build the boundary and initial conditions in this new (x,t,ω) domain for two cases. First we develop conditions for what has historically been viewed as an initial value problem wherein mass appears at $t = 0$ as a function of x. Second we develop conditions for what has historically been a boundary value problem wherein mass is injected at $x = 0$ as a function of t (Sauty, 1980). It is important to note that we do not follow the historical context in either case; instead, in both cases we specify what happens at the age boundary $\omega = 0$. For classical initial value problems we specify the mass occurring at the $\omega = 0$ boundary as a function of space $c_o(x)$ multiplied by the Dirac function $\delta(t)$, as the Dirichlet condition

$$c(x,t,\omega = 0) = c_o(x)\delta(t);\ -\infty < x < \infty,\ 0 \le t, \quad (4)$$

For the classical boundary value problem (Sauty, 1980) specified the cumulative mass injected by time t equal to the total mass contained in the domain $-\infty < x < \infty$; here we specify the rate of mass injection into the domain at the $\omega = 0$ boundary as equivalent to the flow of mass entering the domain physically at $x = 0$:

$$v_\omega c(x,t,\omega = 0) = vc_o(t)\delta(x);\ -\infty < x < \infty,\ 0 \le t.$$

The units of both sides of this equation are mass per volume per time. Defining $c_{in}(t) \equiv \frac{v}{v_\omega}c_o(t)$, we write this boundary condition in Dirichlet form as

$$c(x,t,0) = c_{in}(t)\delta(x)\ \ -\infty < x < \infty,\ 0 \le t, \quad (5)$$

Remaining conditions are conventional. For the limits of the space domain we have

$$\lim_{x\to\pm\infty}\frac{\partial c}{\partial x}(x,t,\omega) = 0;\ 0 \le t,\ 0 \le \omega, \quad (6)$$

and for both cases we adopt a statement of zero mass at initial time,

$$c(x,0,\omega) = 0;\ -\infty < x < \infty,\ 0 < \omega. \quad (7)$$

The foregoing is a novel formulation of two pre-asymptotic dispersion problems when upstream diffusion from the source is allowed. We have recast both the classical initial value and boundary value problems in an explicit age equation: in the first case, instead of assigning the initial data $c_o(x)$ at $t = 0$, we assign it to age $\omega = 0$ and localize the mass at zero time via a Dirac function; and 2. in the second case instead of assigning the boundary influx at the $x = 0$ boundary we specify it at the $\omega = 0$ boundary and localize it at $x = 0$ via the Dirac function $\delta(x)$. This approach gives rise to straightforward development of closed-form solutions (Appendix), and also resolves Taylor's complaint. The solution to the mass conservation equation (3) in the initial value case with Eqs. (4),(6),(7) is (Appendix)

$$c(x,t,\omega) = \delta(t-\omega)e^{-\Lambda(\omega)}\frac{1}{\sqrt{\pi}}\int_{-\infty}^{\infty}e^{-u^2}c_o\left(x - v\omega + u\sqrt{4\tau(\omega)}\right)du. \quad (8)$$

where $\Lambda(\omega) = \int_0^\omega \lambda(u)du$ and $\tau(\omega) = \int_0^\omega D(u)du$. The measurable concentration is the integral of (8) over ω,

$$c_T(x,t) = e^{-\Lambda(t)}\frac{1}{\sqrt{\pi}}\int_{-\infty}^{\infty}e^{-u^2}c_o\left(x - vt + u\sqrt{4\tau(t)}\right)du. \quad (9)$$

In the absence of decay ($\lambda = 0$) Eq. (9) is the same solution as Eq. (7) in Warrick et al. (1972) assuming constant velocity in the latter's case. Given multiple occurrences of solute at the $\omega = 0$ boundary at two sequential times as done in the example from Taghizadeh et al. (2020) described below, (8) provides the solution by superposition. For instance given two appearances of $c_o(x)$ at $t = 0$ and at $t = \Delta$ respectively, then (4) becomes

$$c(x,t,\omega = 0) = c_o(x)(\delta(t) + \delta(t-\Delta)) \quad (10)$$

and then the corresponding solution is Eq. (9) superposed, i.e.,

$$\begin{aligned} c_T(x,t) \ =\ & e^{-\Lambda(t)}\frac{1}{\sqrt{\pi}}\int_{-\infty}^{\infty}e^{-u^2}c_o\left(x - vt + u\sqrt{4\tau(t)}\right)du \\ &+ e^{-\Lambda(t-\Delta)}\frac{1}{\sqrt{\pi}}\int_{-\infty}^{\infty}e^{-u^2}c_o\left(x - v(t-\Delta) + u\sqrt{4\tau(t-\Delta)}\right)du. \end{aligned} \quad (11)$$

Note that this shows a simple case of successful superposition of a single-valued pre-asymptotic dispersion coefficient.

The solution to the mass conservation equation (3) in the now revised boundary-value problem case with Eqs. (5),(6),(7) is (Appendix)

$$c(x,t,\omega) = c_{in}(t-\omega)e^{-\Lambda(\omega)}\frac{1}{\sqrt{4\pi\tau(\omega)}}exp\left(-\frac{(x-v\omega)^2}{4\pi\tau(\omega)}\right). \quad (12)$$

The total (and observable) concentration is the integral of (12) over age,

$$c_T(x,t) = \int_0^\infty c_{in}(t-\omega)e^{-\Lambda(\omega)}\frac{1}{\sqrt{4\pi\tau(\omega)}}exp\left(-\frac{(x-v\omega)^2}{4\pi\tau(\omega)}\right)d\omega. \quad (13)$$

that is the pre-asymptotic generalization of the analogous solution (10.6.13) in Bear (1972) also used in Eq. (13) in Sauty (1980), to which (13) reduces if $\lambda = 0$ and $D(\omega)$ is constant and equal to the asymptotic value of the dispersion coefficient.

4. Initial value problem: Numerical experiment by Taghizadeh et al. (2020)

The purpose of Taghizadeh et al. (2020) (henceforth, "T2020") is to address non-uniform (in directions orthogonal to the flow direction) initial distributions of a solute in 1-D Taylor dispersion, and to address Taylor's criticism that formulations for pre-asymptotic dispersion utilizing time-dependence as in $D(t)$ can lead to multivalued $D(t)$. Our approach does not so far address laterally non-uniform initial distributions but only Taylor's critique.

T2020 specifies four tenets to ensure that a theory for dispersion is well structured: the effective dispersion coefficient should be positive, a function only of diffusion coefficient and velocity field, should reach an asymptotic value over time, and solutions to corresponding advection–dispersion equations should be superposable to avoid Taylor's critique. The fourth tenet is that the solutions to the corresponding advection–dispersion equation should be superposable, which goes directly to Taylor's critique of $D(t)$ forms. We will show that our theoretical model with dispersion as a function of age fits all four of these tenets.

Their approach starts with 3-D advective–diffusive solute transport in pipe Poiseuille flow. The initial condition is specified as one or more solute pulses distributed in x (Case A) as well as in radial direction (Cases B and C). This microscale system is upscaled by a modified volume averaging method that leads to a 1-D transport equation with a time-dependent dispersion coefficient $D^*(t)$ (Eq. (7).3 in T2020), a correction term, $s^*(x,t)$ that depends on initial conditions.

To show how their approach circumvents Taylor's criticism, T2020 present Example 2 (§9.2.1) that involves radially-uniform "initial" conditions, as two sequential solute pulses imposed at an upstream location and at times 0 and 250 min, respectively. Parameter values are given in Table 1 of T2020 and COMSOL is used to solve the microscale equations to obtain solute distributions in cylindrical coordinates and time. The upscaled macroscale model for this example (Eq. (9).6 in T2020) involves two models, each of the form of (1) with $D^*(t)$ replacing $D(t)$ and each with a distinct $s^*(x,t)$ term. The first model is for $0 < t < 250$ min and the second applies at the onset of the appearance of the second initial condition, $t > 250$ min. The initial condition $c_o(x)$ for the first model is a narrow Gaussian distribution over x centered at $x = 0.125$ m, and the initial condition for the second model includes both the profile from the first model at 250 min plus again the reintroduced $c_o(x)$ initial condition, as the second pulse.

In the first model $D^*(t)$ is given by Eq. (7.3) in T2020 for $t > 0$ and $s_1^*(x,t)$ is zero due to the radial uniformity of the first initial condition pulse. The second model for $t > 250$ min is in terms of $t' = t - 250$ min that resets $D^*(t')$ to its initial value equal to the molecular diffusion coefficient. The second model properly times the pre-asymptotic dispersion of the second pulse, but not that of the first pulse which has already undergone 250 min of pre-asymptotic dispersion. This is corrected by the incorporation of $s_2^*(x,t)$ in the second model that treats the first pulse as a non-uniform initial condition at $t' = 0$. This construction allows $D^*(t)$ to be "single valued everywhere in space, including locations where the two solute injections overlap. ...even though the residence times for the two solute injections are not equal, they are described by a single upscaled dispersion coefficient". The $s_2^*(x,t)$ and $D^*(t)$ functions are calculated in MATLAB, then imported into COMSOL that is used to solve the upscaled macroscale models. Figure 16 in T2020 gives the laterally-integrated microscale (solid lines) and macroscale (dots) simulation results, the former of which make up our target data.

We simulated the target data using our Eq. (11) with parameters from T2020's Table 1 as: pipe radius $a = 0.01$ m, mean velocity $v = 10^{-5}$ m/s, diffusion coefficient $D_m = 10^{-9}$ m/s, and $D^*(\omega)$ is T2020's Eq. (7.3) but with ω replacing t (in our age-explicit solution Eq. (8); only after integration over age does the variable t replace ω in (11)). Thus we introduce no fitting parameters. We apply the specified initial value pulse at $t = 0$ and again at $t = 250$ min, via Eq. (10) with the T2020 (Eq. 7.11a) initial condition $c_o(x) = c_o \alpha exp(-(x-\beta_1)^2/\sigma_1^2)$ with $c_o = 1$, $\alpha = 1.1$, $\beta_1 = 0.125$ m, and $\sigma_1 = 0.03$, and with $\Delta = 250$ min.

Fig. 1 shows a good match between our model and the laterally-averaged microscale simulations of T2020, within the confines of upscaled approximate 1D advection–dispersion with pre-asymptotic dispersion coefficient. The perfect match between T2020's macroscale model and the microscale simulation at 250 min results from their accidental use of the latter (microscale averaged solution) as the initial condition for their second macroscale model (personal communication), that also beneficially influenced their subsequent results at 350 and 500 min.

The meticulous study by T2020 to address non-uniform initial conditions illuminates the contradictions inherent in specifying time-dependent dispersion coefficients and achieves a path to superposing solutions for sequential imposed pulses. However, their complex machinery that includes separate macroscale models for each sequential solute injection, each of which is fitted with correction functions that must be numerically computed, involving infinite series of algebraic expressions in Bessel functions, is not needed for approximate solution in those cases where initial conditions vary only in the longitudinal dimension and are otherwise uniform. Our approach serves as a simple means to model pre-asymptotic dispersion while resolving Taylor's critique, using conventional advective–dispersive tooling in a relatively simple single macroscopic equation without correction functions.

5. Boundary value problems on $0 < x$ domains

As noted in the Introduction, the solution of the 1D advection–dispersion equation with time-dependent dispersion coefficient on the half-line $0 < x$ as a boundary value problem with solute condition specified at $x = 0$ has not been found, leading to approximation as an initial value problem on $-\infty < x < \infty$ that involves error that increases with decreasing Péclet number. Thus for moderate to small Péclet number cases it is currently necessary to solve boundary value formulations on $0 < x$ with $D = D(t)$ numerically. Further, the case involving pre-asymptotic dispersion cannot be treated using a time-dependent dispersion coefficient because solute enters the domain continuously over increasing (start-) times. In order to show the utility of our approach we demonstrate how it is used to solve a boundary value problem with pre-asymptotic dispersion, based loosely on the foregoing example from T2020. We simulate transport of two sequential influent pulses in a 1.2 m long pipe of 0.2 m radius at mean velocity $2 \cdot 10^{-5}$ m/s, with a simplified pre-asymptotic dispersion coefficient $D(\omega) = (D_\infty - D_m)(1 - exp(-\omega/2\omega_a)) + D_m$ where D_m is $2 \cdot 10^{-8}$ m^2/ s and D_∞ is $2 \cdot 10^{-6}$ m^2/ s. This exponential model for pre-asymptotic dispersion is suggested with time as independent variable in hydrogeology (e.g., Pickens and Grisak, 1981; Gelhar, 1993; Yates, 1992; Jose and Cirpka, 2004), where ω_a is an advective age scale proportional to characteristic length of flow heterogeneity divided by mean velocity, here taken to be pipe diameter/mean velocity. These values result in a Péclet number advection per diffusion length scales, $Pe \equiv v \cdot a/D_m$ $Pe = 200$ and $\omega_a = 333.33$ min, so that pre-asymptotic dispersion conditions prevail for much of the transport time. The duration of the first pulse is 300 min and after an interval of 100 min a second pulse of duration 200 min is added to the influent. Both of these boundary pulses are specified as Dirichlet boundary conditions of unit concentration $c_o = 1$, as (with t in minutes here)

$$c(x,t,0) = c_o(t)((\Phi(t) - \Phi(t-300)) + (\Phi(t-400) - \Phi(t-600))) \quad 0 \le t \quad (14)$$

where $\Phi(t)$ is the Heaviside step function. To obtain the solution $c(x,t,\omega)$ (2) with (14) is solved by standard implicit finite differences in Matlab, resulting in solute density over space, time, and age, and this solution is numerically integrated in ω to obtain $c_T(x,t)$. The resulting profiles are shown in Fig. 2. For the boundary value problem, the characteristic plots of age, space and density are much more interesting than in the initial value problem case. Here one can observe and keep track of age distributions of solute within the flow field.

The impact of pre-asymptotic dispersion at times comparable to the characteristic time to asymptotic conditions $\omega_a = 333$ min, and the legacy of the pre-asymptotic dispersion at later times, are both apparent in the comparison of our calculated profiles (top row of Fig. 2, solid line) and those calculated with a constant dispersion coefficient (dotted line), even at the moderate Péclet value of 200. The contour and surface plots illustrate how our additional advection in the age dimension distributes the solute emanating from a boundary influx over age, allowing the dispersive flux to be computed differently per every

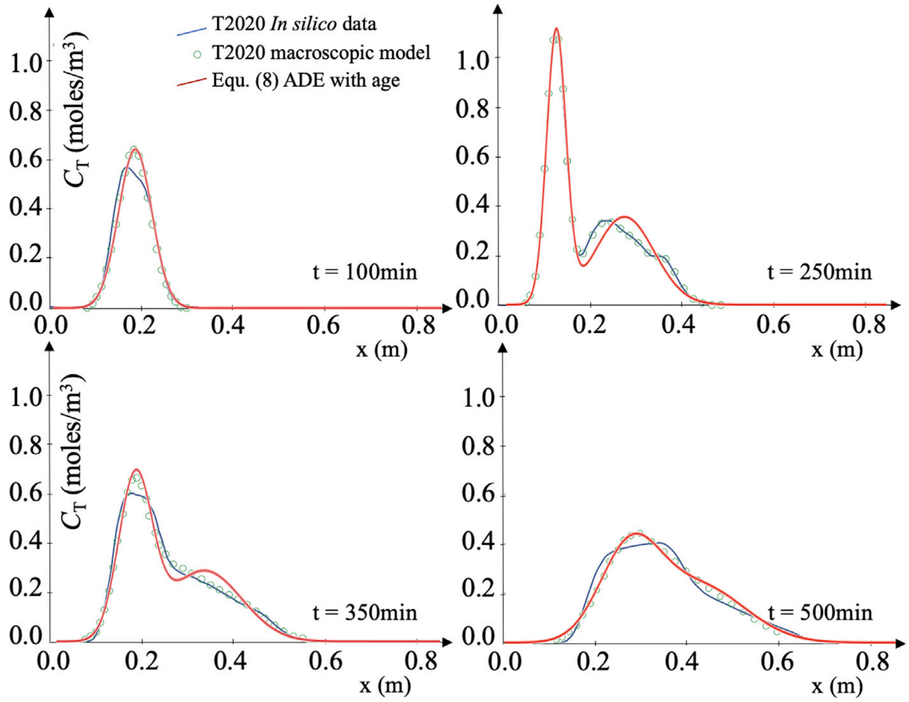

Fig. 1. Simulations of Example 2 of T2020 Section 9.2.1 showing solute profiles at four times. In silico data (blue line) represent the laterally-averaged microscopic simulation and is the target. Green circles show simulation by T2020 macroscopic model equation 9.6. Simulation using superposed solution (11) of age-structured advection–dispersion ((2) with initial and boundary conditions described in Section 4) is in red.

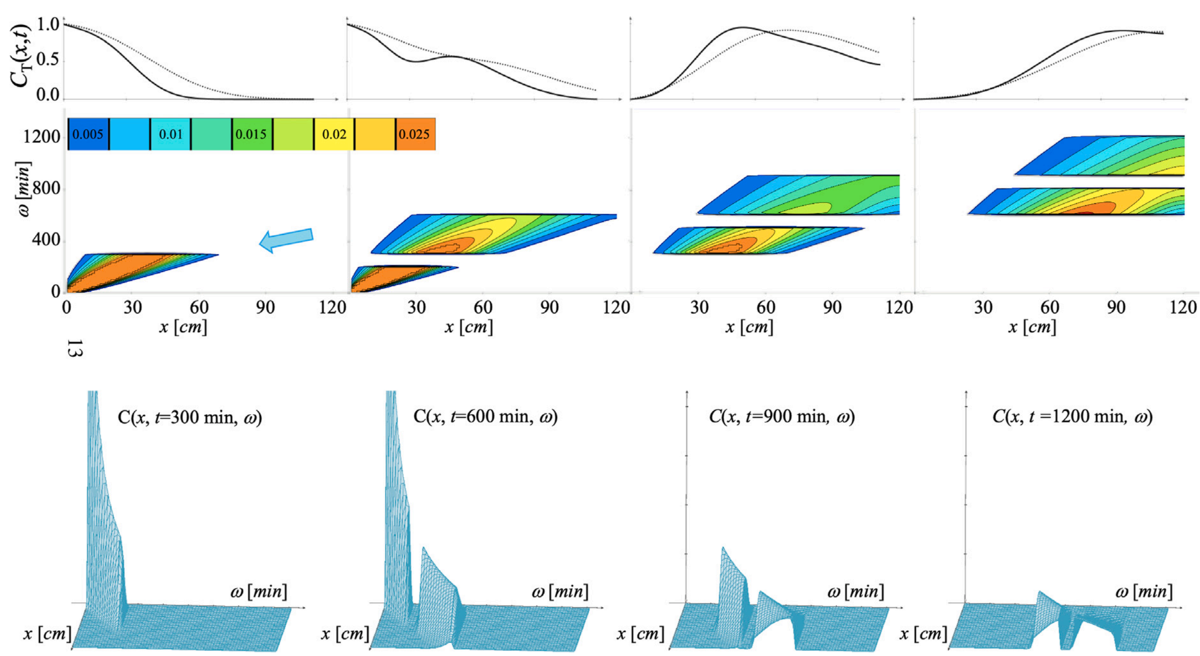

Fig. 2. Illustrated solution to 1-D advective–dispersive transport with age as independent variable (2). Transport occurs at Pe = 200 in a 120 cm long column at steady mean velocity 0.12 cm/min, with characteristic age ω_a = 333 min; other properties described in text. Panel columns show solute distribution at 300, 600, 900, and 1200 min respectively. Top row: concentration profiles $c_T(x,t)$ (solid line, (2) integrated over ω), with constant $D = D_\infty$ case (dotted line, solution in Ogata and Banks (1961)) for comparison. Middle row: contour plots of $c(x,t,\omega)$ (inset is heatmap scale, truncated at 0.025 to accommodate color differentiation at later times). Bottom row figures are surface plots of $c(x,t,\omega)$. The blue arrow in the 300 min contour plot in the second row shows the point of view for the surface plots at the bottom.

age value ω. This construction allows solutes that overlap in space at any given time to be assigned different dispersion coefficient values depending on the solute age. The two pulses in this example overlap considerably in space as can be seen from the contour plots, and the different extent of dispersion for solute in either pulse is apparent in the nonuniform solute distributions over age shown in the surface plots.

6. Summary and conclusions

Local forms of mathematical models for advective–dispersive transport including pre-asymptotic regimes has to date been addressed by use of a dispersion coefficient that depends in general on time for initial value problems or on spatial scale for boundary value problems. Analyses of superposition for both formulations leads to problematic multi-valued nature of the dispersion coefficient as noted for the time-dependent case in Taylor (1959). Following Gurung and Ginn (2020) we address this issue by including exposure time to flow (age) as an independent variable in the transport equation. Incorporating age explicitly and treating the dispersion coefficient as a function of age honors the dispersive flux and inherently retains superposition of solute densities distributed in age via *a posteriori* integration over the age dimension. In our example from T2020 we show how this works, without introduction of any fitting parameters. Our second example demonstrates numerical solution feasibility given the expression for the dispersion coefficient that itself may involve fitting parameters. New closed-form solutions are found for the 1-D initial value (Eq. (8)) and boundary value (Eq. (13) problems.

The only approaches to the pre-asymptotic dispersion problem that are local and that address Taylor's critique are the method presented here and that of T2020. These begin with a fluid mechanical setting and known $D(\omega)$, and develop solutions to the advective–dispersive transport problem. The complexity in the approach of T2020 derives from the need to use a single-valued $D(t)$ function when considering the profiles emanating from sequential imposed pulses in the same simulation. This can be seen by noting (cf. Section 1) that one could in fact solve the example without $s^*(x,t)$ terms by separately calculating the profiles from the first (at $t = 0$) and second (at $t' = 0$) imposed initial pulses, and superposing the obtained solutions on the same t-axis. (In the T2020 example used here, the role of $s_2^*(x,t)$ is to undo the impact of the inclusion of the $t = 250$s solution for the first profile in the initial condition for the second model at $t' = 0$). The approach of T2020 to address non-uniform initial conditions in 3-D (the authors' main purpose) do indeed provide a path to dealing with sequential imposed pulses, but this machinery is not needed for the superposition problem if true initial conditions vary only in the axial dimension and if one includes age.

Celebrated among nonlocal methods are the CTRW (Dentz et al., 2004) and correlated CTRW (Le Borgne et al., 2011) approaches, that begin with a fluid mechanical-based specification of usually independent particle jump time and space interval frequency distribution functions independent of time or space. The resulting random walk model gives rise to particle tracking schemes or to integrodifferential advection–dispersion equations wherein the advection and dispersion terms are both involved in a convolution with a memory function (e.g., (Boano et al., 2007)). These approaches can be configured with sufficiently truncated power-law time interval distributions so that resulting effective dispersion coefficients reach asymptotic constant values (e.g., (Dentz et al., 2004; Talon et al., 2023)) but the method has not yet been configured for a pre-specified $D(\omega)$, nor to address Taylor's critique, to the authors' knowledge. Separately, the CTRW particle jump interval frequency distribution function generally combines transport with non-transport, that is, trapping time intervals, a feature common to all the above. In the case of Boano et al. (2007) when these trapping events are removed, the resulting model is the asymptotic (constant D) advection–dispersion equation.

Here we use age to design a local, Eulerian-frame, deterministic modeling of Fickian transport through both the transition from pre-asymptotic to asymptotic regimes the dispersion coefficient expression. In principle the use of age as independent variable allows such constructions generally in a way that solves Taylor's complaint and affords superposition. The incorporation of reactions and multiple components can in principle be done following the usual approaches for Eulerian transport models. The approach also affords distinction between pre-asymptotic dependence of dispersion coefficient on age and genuine dependence of dispersion on time through transience in velocity metrics. For instance, in the context of transport in a porous medium where D is often expressed as the product of a dispersivity α and a function of the velocity (e.g. in 1D homogeneous media, where $D = \alpha f(v(t))$), the age dependence would be assigned to α alone. Incorporation of age in transport in the present context honors the four tenets proposed in T2020: the effective dispersion coefficient remains positive, depends only on diffusion coefficient and velocity field, reaches an asymptotic value over time (here, age); and the solution to the advection–dispersion equation is superposable, here through integration of the realized solution over the age dimension.

In this work we are implementing existing formulations of models that use a pre-asymptotic one-dimensional dispersion coefficient, in which we suggest replacement of time t with age ω, in general. The limitations of the present approach as noted earlier are the restriction to steady flow, and the requirement for an upscaled one-dimensional $D(t)$ that adequately describes longitudinal dispersion in the upscaled transport model. This in turn requires explicit expressions for the full-dimensional ("microscopic") flow field as well as additional assumptions involved in the particular upscaling of the transport process from the original full-dimensional representation to the effective one-dimensional model. For instance, various $D(t)$ forms are available for pipes (Gill and Sankarasubramanian, 1970), conduits with unsteady flow (Vedel and Bruus, 2012), rivers (Wang et al., 2012), some aquifers (Dentz et al., 2000; Dentz and Carrera, 2007); and each of these results are attached to assumptions about the flow field that can limit accurate application (e.g. Wang et al. (2012) require Poiseuille flow). Additional assumptions associated with the mathematical upscaling appear in these particular cases and more cited in the Introduction, where developers have derived $D(t)$ expressions on which we here rely. Finally we have paid for locality by invention of an additional dimension, that of age ω, and so problems involving N space dimensions will result in numerical schemes involving $N + 1$ dimensions in addition to time (e.g., (Woolfenden and Ginn, 2009)), that may encounter computational limits.

CRediT authorship contribution statement

Deviyani Gurung: Investigation, Formal analyses, Software, Visualization, Writing – original draft. **Mohammad Aghababaei:** Methodology, Software. **Timothy R. Ginn:** Conceptualization, Formal analyses, Methodology, Supervision, Writing – original draft, Writing – revision, Project administration, Funding acquisition, Visualization.

Declaration of competing interest

The authors declare the following financial interests/personal relationships which may be considered as potential competing interests: Timothy R. Ginn reports financial support was provided by National Science Foundation CBET. Timothy R. Ginn reports financial support was provided by National Science Foundation HYD.

Data availability

No new data used, example problem involved data from another publication.

Acknowledgments

We thank the authors of T2020 for helpful discussions and useful references, and for open sharing of their COMSOL codes, and Marco Dentz of the Spanish National Research Council for helpful discussion. We also thank the Editor, Associate Editor and three anonymous reviewers for constructive reviews that significantly improved the paper. This research was supported by NSF/HYD project 2142165, Collaborative Research: Informing River Corridor Transport Modeling by Harnessing Community Data and Physics-Aware Machine Learning; by NSF/CBET project 1855609, Collaborative Research: Influence of drinking water chemical composition on biofilm properties and toxic disinfection byproduct formation: an experimental and modeling study; and by the Boeing Fund in Environmental Engineering at WSU.

Appendix. Details of the closed-form solutions

Here we show details of the solution of Eq. (3), for the case where the space domain is $-\infty < x < \infty$, first for the 'Age-initial value problem' where the distribution of solute concentration over x is specified at time $t = 0$ and age $\omega = 0$, and then for the 'age-boundary value problem' where solute is injected as a function of time at $x = 0$ and at age $\omega = 0$.

A.1. Age-initial value problem

For completeness we restate the model. The conservation of mass over space, time and age is

$$v_\omega \frac{\partial c}{\partial \omega} + \frac{\partial c}{\partial t} + v\frac{\partial c}{\partial x} - D(\omega)\frac{\partial^2 c}{\partial x^2} = -\lambda(\omega)c;\ -\infty < x < \infty, 0 < t,\ 0 < \omega, \quad \text{(A.1)}$$

where $v_\omega = 1$, with age-initial (Dirichlet-type) condition

$$c(x, t, \omega = 0) = c_o(x)\delta(t);\ -\infty < x < \infty,\ 0 \le \omega, \quad \text{(A.2)}$$

boundary conditions in space

$$\lim_{x\to\pm\infty} \frac{\partial c}{\partial x}(x, t, \omega) = 0;\ 0 \le t,\ 0 \le \omega, \quad \text{(A.3)}$$

and initial condition

$$c(x, 0, \omega) = 0;\ -\infty < x < \infty,\ 0 \le \omega. \quad \text{(A.4)}$$

Making the change of variables

$$\begin{aligned} x &= x' + vt' & x' &= x - v\omega \\ \omega &= t' & t' &= \omega \\ t &= t' + \omega' & \omega' &= t - \omega \end{aligned}$$

leads to a family of equations in ω' for $c(x', t'; \omega')$ governed by

$$\frac{\partial c}{\partial t'} - D(t')\frac{\partial^2 c}{\partial x'^2} = -\lambda(t')c;\ \ -\infty < x' < \infty,\ 0 < t', 0 < \omega', \quad \text{(A.5)}$$

with

$$\begin{aligned} c(x', 0; 0) &= 0; & -\infty < x' < \infty, \\ c(x', 0, \omega') &= c_o(x')\delta(\omega'); & -\infty < x' < \infty,\ 0 < \omega', \\ \lim_{x'\to\pm\infty} \frac{\partial c}{\partial x'}(x', t', \omega') &= 0; & 0 \le t',\ 0 \le \omega'. \end{aligned}$$

Applying the integration factor method with $c = fe^{-\Lambda(t')}$ where $\Lambda(t') = \int_0^{t'} \lambda(u)du$ converts this system to

$$\frac{\partial f}{\partial t'} - D(t')\frac{\partial^2 f}{\partial x'^2} = 0;\ \ -\infty < x' < \infty,\ 0 < t', 0 < \omega', \quad \text{(A.6)}$$

$$\begin{aligned} f(x', 0; 0) &= 0; & -\infty < x' < \infty, \\ f(x', 0; \omega') &= c_o(x')\delta(\omega'); & -\infty < x' < \infty,\ 0 < \omega', \\ \lim_{x\to\pm\infty} \frac{\partial f}{\partial x'}(x', t'; \omega') &= 0; & 0 \le t',\ 0 \le \omega'. \end{aligned}$$

The further change of variables

$$\tau = \int_0^{t'} D(u)du \quad \text{(A.7)}$$

yields

$$\frac{\partial f}{\partial \tau} - \frac{\partial^2 f}{\partial x'^2} = 0;\ \ -\infty < x' < \infty,\ 0 < \tau, 0 < \omega', \quad \text{(A.8)}$$

$$\begin{aligned} f(x', \tau = 0; 0) &= 0; & -\infty < x' < \infty, \\ f(x', 0; \omega') &= c_o(x')\delta(\omega') & -\infty < x' < \infty,\ 0 < \omega'. \\ \lim_{x\to\pm\infty} \frac{f}{\partial x'}(x', \tau; \omega') &= 0; & 0 \le \tau,\ 0 \le \omega', \end{aligned}$$

The solution can be adapted following Warrick et al. (1972) (following Carslaw and Jaeger (1959) p. 53), to write

$$f(x', t'; \omega') = \delta(\omega')\frac{1}{\sqrt{\pi}}\int_{-\infty}^{\infty} e^{-u^2} c_o\left(x' + u\sqrt{4\tau(t')}\right) du. \quad \text{(A.9)}$$

Reversing the integration factor change of variables, we obtain

$$c(x', t'; \omega') = \delta(\omega')e^{-\Lambda(t')}\frac{1}{\sqrt{\pi}}\int_{-\infty}^{\infty} e^{-u^2} c_o\left(x' + u\sqrt{4\tau(t')}\right) du.$$

and reversing the original change of variables yields

$$c(x, t, \omega) = \delta(t - \omega)e^{-\Lambda(\omega)}\frac{1}{\sqrt{\pi}}\int_{-\infty}^{\infty} e^{-u^2} c_o\left(x - v\omega + u\sqrt{4\tau(\omega)}\right) du. \quad \text{(A.10)}$$

where $\Lambda(\omega) = \int_0^\omega \lambda(u)du$ and $\tau(\omega) = \int_0^\omega D(u)du$. Finally, the measurable concentration is the integral of (A.10) over ω,

$$c_T(x, t) = e^{-\Lambda(t)}\frac{1}{\sqrt{\pi}}\int_{-\infty}^{\infty} e^{-u^2} c_o\left(x - vt + u\sqrt{4\tau(t)}\right) du. \quad \text{(A.11)}$$

A.2. Age-boundary value problem

This system is identical to (A.1)–(A.5) above but we replace the Dirichlet condition at $\omega = 0$ (A.2) with the Neumann condition

$$v_\omega c(x, t, 0) = vc_o(t)\delta(x);\ -\infty < x < \infty,\ 0 \le t.$$

The units of both sides of this equation are mass per volume per time. Defining $c_{in}(t) \equiv \frac{v}{v_\omega}c_o(t)$, we write this boundary condition in Dirichlet form as

$$c(x, t, 0) = c_{in}(t)\delta(x)\ \ -\infty < x < \infty,\ 0 \le t. \quad \text{(A.12)}$$

Making the same change of variables as above leads to again (A.5) but now with

$$\begin{aligned} c(x', 0; 0) &= 0; & -\infty < x' < \infty, \\ c(x', 0, \omega') &= c_{in}(\omega')\delta(x'); & -\infty < x' < \infty,\ 0 < \omega', \\ \lim_{x'\to\pm\infty} \frac{\partial c}{\partial x'}(x', t', \omega') &= 0; & 0 \le t',\ 0 \le \omega'. \end{aligned}$$

Applying the same integration factor method with $c = fe^{-\Lambda(t')}$ yields

$$\frac{\partial f}{\partial t'} - D(t')\frac{\partial^2 f}{\partial x'^2} = 0;\ \ -\infty < x' < \infty,\ 0 < t', 0 < \omega', \quad \text{(A.13)}$$

$$\begin{aligned} f(x', 0; 0) &= 0; & -\infty < x' < \infty, \\ f(x', 0; \omega') &= c_{in}(\omega')\delta(x'); & -\infty < x' < \infty,\ 0 < \omega', \\ \lim_{x\to\pm\infty} \frac{\partial f}{\partial x'}(x', t'; \omega') &= 0; & 0 \le t',\ 0 \le \omega', \end{aligned}$$

and the same further change of variables

$$\tau = \int_0^{t'} D(u)du \quad \text{(A.14)}$$

gives in this case

$$\frac{\partial f}{\partial \tau} - \frac{\partial^2 f}{\partial x'^2} = 0;\ \ -\infty < x' < \infty,\ 0 < \tau, 0 < \omega', \quad \text{(A.15)}$$

$$\begin{aligned} f(x', \tau = 0; 0) &= 0; & -\infty < x' < \infty, \\ f(x', 0; \omega') &= c_{in}(\omega')\delta(x') & -\infty < x' < \infty,\ 0 < \omega'. \\ \lim_{x\to\pm\infty} \frac{\partial f}{\partial x'}(x', \tau; \omega') &= 0; & 0 \le \tau,\ 0 \le \omega', \end{aligned}$$

Then the solution

$$f(x', t'; \omega') = c_{in}(\omega')\frac{1}{\sqrt{\pi}}\int_{-\infty}^{\infty} e^{-u^2} \delta\left(x' + u\sqrt{4\tau(t')}\right) du. \quad \text{(A.16)}$$

is obtained. Reversing the integration factor variable change, we obtain

$$c(x', t'; \omega') = c_{in}(\omega')e^{-\Lambda(t')}\frac{1}{\sqrt{\pi}}\int_{-\infty}^{\infty} e^{-u^2} \delta\left(x' + u\sqrt{4\tau(t')}\right) du.$$

and reversing the original change of variables yields

$$c(x, t, \omega) = c_{in}(t - \omega)e^{-\Lambda(\omega)}\frac{1}{\sqrt{\pi}}\int_{-\infty}^{\infty} e^{-u^2} \delta\left(x - v\omega + u\sqrt{4\tau(\omega)}\right) du.$$

Using the rules for Dirac functions of functions,

$$c(x,t,\omega) = c_{in}(t-\omega)e^{-\Lambda(\omega)}\frac{1}{\sqrt{4\pi\tau(\omega)}}exp\left(-\frac{(x-\upsilon\omega)^2}{4\pi\tau(\omega)}\right). \tag{A.17}$$

where $\Lambda(\omega) = \int_0^{\omega}\lambda(u)du$ and $\tau(\omega) = \int_0^{\omega}D(u)du$. Integration of (A.17) over ω from 0 to t yields the measurable concentration $c_T(x,t)$. Note that in the case where $c_o(t) = c_o\Phi(t)$ where $\Phi(t)$ is the Heaviside function, and where $\lambda = 0$ this integration yields

$$c_T(x,t) = \frac{\upsilon}{\upsilon_{\omega}}c_o\int_0^t\frac{1}{\sqrt{4\pi\tau(\omega)}}exp\left(-\frac{(x-\upsilon\omega)^2}{4\pi\tau(\omega)}\right)d\omega. \tag{A.18}$$

References

Aris, 1956. On the dispersion of a solute in a fluid flowing through a tube. Proc. Roy. Soc. A 235, 67–77.

Barry, D.A., Sposito, G., 1989. Analytical solution of a convection-dispersion model with time-dependent transport coefficients. Water Resour. Res. 25 (12), 2407–2416.

Bear, J., 1972. Dynamics of Fluids in Porous Media. Elsevier, New York, p. 764.

Boano, F., Packman, A.I., Cortis, A., Revelli, R., Ridolfi, L., 2007. A continuous time random walk approach to the stream transport of solutes. Water Resour. Res. 43 (W10425).

Carslaw, H.S., Jaeger, J.C., 1959. Conduction of Heat in Solids, second ed. Clarendon Press, Oxford, p. 510.

Charbeneau, R.C., 2000. Groundwater Hydraulics and Pollutant Transport. Prentice-Hall Inc, Upper Saddle River, NJ, p. 593.

Corey, J.C., Hawkins, R.H., Overman, R.F., Green, R.E., 1970. Miscible displacement measurement within laboratory columns using the gamma photoneutron method. Soil Sci. Soc. Am. Proc. 34, 854–858.

Dagan, G., 1984. Solute transport in heterogeneous porous formations. J. Fluid Mech. 145, 151–177.

Dagan, G., 1987. Theory of solute transport by groundwater. Ann. Rev. Fluid Mech. 19, 183–215.

Delhez, E.J.M., Campin, J.-M., Hirst, A.C., Deleersnijder, E., 1999. Toward a general theory of age in ocean modelling. Ocean Model. 1 (1), 17–27.

Deng, B., Qiu, Y., 2012. Comment on analytical solutions to one-dimensional advection–diffusion equation with variable coefficients in semi-infinite media by kumar, a., jaiswal, d.k., kumar, n., j. hydrol., 2010 380: 330–337. J. Hydrol. 424-425, 278–279.

Dentz, M., Carrera, J., 2007. Mixing and spreading in stratified flow. Phys. Fluids 19, 017107, 17 pages.

Dentz, M., Cortis, A., Berkowitz, B., 2004. Time behavior of solute transport in heterogeneous media: transition from anomalous to normal transport. Adv. Wat. Resour. 127 (2), 155–173.

Dentz, M., Kinzelbach, H., Attinger, S., Kinzelbach, W., 2000. Temporal behavior of a solute cloud in a heterogeneous porous medium 1. Point-like injection. Water Resour. Res. 36 (12), 3591–3604.

Fischer, H.B., 1967. The mechanics of dispersion in natural streams. ASCE J. Hydraul. Div. 93 (6), 187–216.

Fried, J.J., Combarnous, M.A., 1971. Dispersion in porous media. Adv. Hydrosci. 7, 169–282.

Gelhar, L.W., 1993. Stochastic Subsurface Hydrology. Prentice-Hall Inc, Englewood Cliffs, NJ, p. 390.

Gill, W.M., 1967. A note on the solution of transient dispersion problems. Proc. Roy. Soc. A 316, 335–339.

Gill, W.M., Sankarasubramanian, R.S., 1970. Exact analysis of unsteady convective diffusion. Proc. Roy. Soc. A 298, 341–350.

Ginn, T.R., 1999. On the distribution of generalized exposure-time in groundwater flow and reactive transport: Foundations; formulations for groundwater age, geochemical heterogeneity, and biodegradation. Water Resour. Res. 35, 1395–1408.

Ginn, T.R., 2009. Generalization of the multirate basis for time-convolution to unequal forward and reverse rates and connection to reactions with memory. Water Resour. Res. 45 (12419).

Ginn, T.R., Loge, F.J., 2007. Dose-structured population dynamics. Math. Biosci. 208 (1), 325–343.

Ginn, T.R., Schreyer, L.G., 2023. Compartment models with memory. SIAM Rev. 65 (3), 774–805.

Ginn, T.R., Schreyer, L., Zamani, K., 2017. Phase exposure-dependent exchange. Water Resour. Res. 53, 619–632.

Gurung, D., Ginn, T.R., 2020. Mixing ratios with age: application to preasymptotic one-dimensional equilibrium bimolecular reactive transport in porous media. Water Resour. Res. 56 (7), e2020WR027629.

Guven, O., Molz, F.J., Melville, J.G., 1984. An analysis of dispersion in a stratified aquifer. Water Resour. Res. 20 (10), 1337–1354.

Han, N.-W., Bhakta, J., Carbonell, R.G., 1985. Longitudinal and lateral dispersion in packed beds: Effect of column length and particle size distribution. AIChE J. 31 (2), 277–288.

Jose, S.C., Cirpka, O.A., 2004. Measurement of mixing-controlled reactive transport in homogeneous porous media and its prediction from conservative tracer test data. Envi. Sci. Technol. 38, 2089–2096.

Le Borgne, T., Bolster, D., Dentz, M., de Anna, P., Tartakovsky, A., 2011. Effective pore-scale dispersion upscaling with a correlated continuous time random walk approach. Water Resour. Res. 47 (12), 10.

Ogata, A., Banks, R.B., 1961. A solution of the differential equation of longitudinal dispersion in porous media. Geol. Surv. Prof. Paper 411-A.

Pasmanter, R.A., 1985. Exact and approximate solutions of the convection–diffusion equation. Q. J. Mech. Appl. Math. 38 (1), 1–26.

Pérez Guerrero, J.S., Skaggs, T.H., 2010. Analytical solution for one-dimensional advection–dispersion transport equation with distance-dependent coefficients. J. Hydrdol. 390 (1–2), 57–65.

Pickens, J.F., Grisak, G.E., 1981. Modelling of scale dependent dispersion in hydrogeological systems. Water Resour. Res. 17, 1701–1711.

Sauty, J.-P., 1980. An analysis of hydrodispersive transfer in aquifers. Water Resour. Res. 16 (1), 145–158.

Sengör, S.S., Barua, S., Gikas, P., Ginn, T.R., Peyton, B.M., Sani, R., Spycher, N., 2009. Influence of heavy metals on microbial growth kinetics including lag time: Mathematical modeling and experimental verification. Environ. Toxicol. Chem. 28 (10), 2020–2029.

Seo, I.W., Cheong, T.S., 1998. Predicting longitudinal dispersion coefficient in natural streams. ASCE J. Hydraul. Eng. 124 (1), 25–32.

Smith, R., 1981. A delay-diffusion description for contaminant dispersion. J. Fluid Mech. 105 (part 9), 469–486.

Taghizadeh, E., Valdés-Parada, F.J., Wood, B.D., 2020. Preasymptotic Taylor dispersion: evolution from the initial condition. J. Fluid Mech. 889 (A5), A5-1-A5-64.

Talon, L., Ollivier-Triquet, E., Dentz, M., Bauer, D., 2023. Transient dispersion regimes in heterogeneous porous media: On the impact of spatial heterogeneity in permeability and exchange kinetics in mobile–immobile transport. Adv. Water Resour. 174, 104425.

Taylor, G.I., 1953. Dispersion of soluble matter in solvent flowing slowly through a tube. Proc. Roy. Soc. A 219, 186–203.

Taylor, G.I., 1954. The dispersion of matter in turbulent flow through a pipe. Proc. Roy. Soc. A 223, 446–468.

Taylor, G.I., 1959. The present position in the theory of turbulent diffusion. Adv. Geophys. 6, 101–112.

Vedel, S., Bruus, H., 2012. Transient Taylor-Aris dispersion for time-dependent flows in straight channels. J. Fluid Mech. 691, 95–122.

Wang, L., Cardenas, M.B., Deng, W., Bennett, P., 2012. Theory for dynamic longitudinal dispersion in fractures and rivers with Poiseuille flow. Geophys. Res. Lett. 39, L05401C.

Warrick, A.W., Kichen, J.H., Thames, J.L., 1972. Solutions for miscible displacement of soil water with time-dependent velocity and dispersion doefficients. Soil Sci. Soc. Am. Proc. 36, 863–867.

Woolfenden, L., Ginn, T.R., 2009. Modeled ground water age distributions. Groundwater 47, 547–557.

Yates, S.R., 1992. An analytical solution for one-dimensional transport in porous media with an exponential dispersion function. Water Resour. Res. 28 (8), 2149–2154.